Indian Journal of Chemistry
Vol. 59A, October 2020, pp. 1434-1441

Guests mediated supramolecule-modified gold nanoparticles network for mimic enzyme application

Jialin Zhao[a,b#], Zhijuan Niu[c#], Xing Huang[b], Xiaojun Hu[b], Shouwei Gao[d], Kwangnak Koh[e] & Hongxia Chen[b]*

[a]State Key Laboratory of Dairy Biotechnology, Bright Dairy & Food Co. Ltd, Shanghai 200444, PR China

[b]Laboratory of Biosensing Technology, School of Life Sciences, Shanghai University, Shanghai 200444, PR China

[c]Guangdong Provincial Key Laboratory of Environmental Pollution and Remediation Technology, School of Environmental Science and Engineering, Sun Yat-sen University, Guangzhou, 510275, China

[d]School of Mechatronic Engineering and Automation, Shanghai University, Shanghai, 200444, P. R. China

[e]Institute of General Education, Pusan National University, Pusan 609735, Republic of Korea

Email: hxchen@shu.edu.cn

Received 14 January 2020; revised and accepted 15 June 2020

Supramolecules mediated porous metal nanostructures are meaningful materials because of their specific properties and wide range of applications. Here, we describe a general and simple strategy for building Au-networks based on the guest-induced 3D assembly of Au nanoparticles (Au-NPs) resulted in host-guest interaction resolved sulfonatocalix[4]arene (pSC_4)-modified Au-NPs aggregate. The diverse guest molecules induced different porous network structures resulting in their different oxidize ability toward glucose. Among three different kinds of guest, hexamethylenediamine-pSC_4-Au-NPs have high sensitivity, wide linear range and good stability. By surface characterization and calculating the electrochemical properties of the Au-NPs networks modified glassy carbon electrodes, the giving Au-NPs network reveals good porosity, high surface areas and increased conductance and electron transfer for the electrocatalysis. The synthesized nano-structures afford fast transport of glucose and ensure contact with a larger reaction surface due to high surface area. The fabricated sensor provides a platform for developing a more stable and efficient glucose sensor based on supramolecules mediated Au-NPs networks.

Keywords: Au-NP network, Glucose sensing, *para*-sulfonatocalix[4]arene, Mimic enzyme, Nanoparticle assembly

Due to the important applications of nanostructures in electronics, photovoltaics, optics, sensing, catalysis and biomedical applications, the assembly of colloidal nanocrystals into nanostructured materials with macroscopic dimensions has attracted more and more research interest.[1-4] Significant efforts have been made in the self-assembly or directional assembly of nanoparticles (NPs) into one, two and three dimensions. This concept provides a bottom-up, controllable approach to material projects and extends the range of potential applications.[5-8] However, it is still a challenge to incorporate nanosized entities with their unique electronic, magnetic and/or optical properties into materials having macroscopic dimensions that are easy to process and manipulate. Recently, gels made from various semiconductor and metal NPs available in colloidal solutions have been shown to provide such a route.[9-10] For example, ions are reduced in situ to form Ag or Au-NPs with a degree of organization on the gel nanofibers.[11] These hybrid materials are electrically conductive due to implanted NPs and can be treated as modified electrodes.[12,13]

It is well-known that the composition and structure of NPs and the properties of NPs modified electrode interface can have an effect on the electrochemical properties of NPs-functionalized electrodes, which are critical in photocatalytic, electrocatalytic and electrochemical sensing applications.[14-18] Au-NPs tend to form large-sized aggregates under various conditions, such as salt, pH, oxidation and temperature, which inhibit the construction of three-dimensional (3D) network nanostructures. Up to now, Au-networks with nano-metal skeletons have been assembled by an immediate gel method and in particular their applications are still largely undiscovered and a huge challenge. Different strategies have been devised, such as adjustable, controllable and uniform interface structures.[19-21] The

[#] Authors contribute equally

study of Au-NPs and various nanostructures has been extensively studied due to their wide application and fascinating properties in biomedicine, nanoelectronics, catalysis, sensing, etc.[22-27] Eychmüller *et al.* have made significant progress in Au aerogel based on β-cyclodextrin modification to overcome pre-aggregation[13]. However, chemical regulation of nanomaterial assembly remains challenging.

In the case of supramolecular functionalized Au-NPs, several assembly strategies introduce interactions between guest molecules and supramolecular functionalized the surfaces of Au-NPs[28,29]. Yang *et al.*[21] reported an approach of 3D nanostructure in liquid phase based on the assembly of guest molecules. Tang *et al.*[30] constructed a simple hydrogen peroxide biosensor based on the electrocatalysis of hemoglobin immobilized on gold NPs/1,6-diaminohexane modified glassy carbon electrode (GCE). However, to the best of our knowledge, there is no assembly strategy based on the interaction of guest molecules with supramolecular modified Au-NPs surfaces for glucose sensing. Glucose testing is extremely important in the clinical diagnosis of diabetic patients. The most commonly used glucose sensor is based on enzymes.[31] At present, nano-mimetic enzymes have become a research hotspot due to their advantages, such as easy synthesis, stability, wide pH and temperature range. In this contribution, we presented on a moderate strategy for providing para-sulfonatocalix[4]arene-modified Au-NPs (pSC_4-Au-NPs) networks composed of 3D-network structures by 1,6-diaminohexane hexanediamine (HMD) induced assembly of pSC_4-Au-NPs (Scheme 1). Here, the HMD acts as an effective linker for the controlled assembly of pSC_4-Au-NPs into a network through the host-guest interaction with pSC_4. This synthetic procedure is simple, rapid and versatile compared to pre-aggregation of NPs method. The provided pSC_4-Au-NPs network exhibits high porosity and large active surface area. Electrochemical results indicate that the pSC_4-Au-NPs network linked by HMD greatly promotes the catalytic process. This approach provides a platform for the development of more stable and efficient glucose sensors based on guests mediated supramolecule-modified Au-NPs networks.

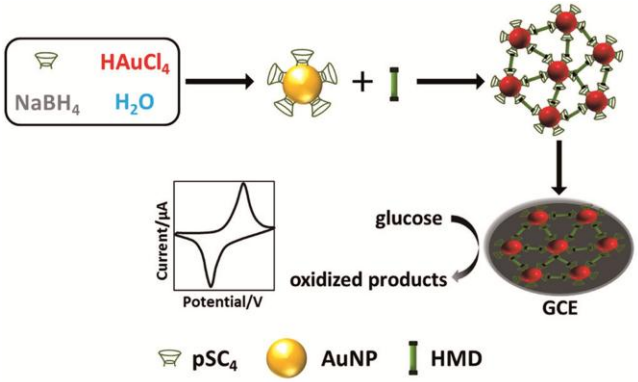

Schematic illustration of the mechanisms for the synthesis of pSC4-Au-NPs, pSC4-Au-NPs aggregation induced by host–guest recognition, and evaluation for electrocatalyst

Scheme 1

Materials and Methods

Reagents and materials

Hydrogen tetrachloroaurate trihydrate ($HAuCl_4 \cdot 3H_2O$), *β*-D-(+)-glucose, dopamine hydrochloride, paraquat and L-ascorbic acid were purchased from Sigma-Aldrich, Inc. (St. Louis, USA). Sodium borohydride ($NaBH_4$), 1,4-diaminobutane and 1,8-diaminooctane were purchased from Aladdin, Inc. (Shanghai,China). 1,6-diaminohexane/ hexanediamine was purchased from Sinopharm Chemical Reagent Co. Ltd, (Shanghai, China). *para*-Sulfonatocalix[4]arene was purchased from TCI (Shanghai) Development Co. Ltd, (Shanghai, China). For the electrocatalytic experiments, a NaOH solution (0.1 or 1 M) was used as supporting electrolyte. Other chemicals were of analytical grade, and all solutions were intended with deionized water purified with a Milli-Q distillation system (Branstead, USA) to a decided resistance of 18.2 MΩ·cm.

pSC_4-Au NPs synthesis

First, all glasswares were purified with freshly prepared aqua regia (HCl/HNO_3 = 3:1) and rinsed thoroughly in deionized water.The pSC_4-Au-NPs was synthesized on the basis of the reported strategy with modification.[32] In summary, pSC_4 (2 mL, 2×10^{-3} mol/L) and $HAuCl_4$ solutions (2 mL, 1.25×10^{-3} mol/L) were added to 96 mL of water in file at room temperature. After stirring for 25 min in the dark, freshly prepared $NaBH_4$ solution (2 mL, 2×10^{-3} mol/L) was added into the mixture solution rapidly, and then continues stirring for 2 h in the dark. A regulatory color change from bright yellow to dark brown and light red was observed. The pSC_4-Au-NPs colloids were ultimately obtained. The resulting solution was stored at 4 °C in an amber bottle. UV–visible absorption, FTIR and SEM techniques were used to characterize the synthetic pSC_4-Au NPs.

Preparation of pSC_4-Au NPs networks

A network from pSC_4-Au NPs was prepared by adding 10 μL of HMD solution (10 mM) to 90 μL of

pSC_4-modified Au colloid to produce a final concentration of 1 mM. After gently shaking, 100 μL of the above solution was obtained, followed by precipitating at 4 °C. Other guest, PQ or dopamine-induced pSC_4-Au-NPs assembly was obtained by a system similar to that described above.

Electrocatalytic experiments

Traditional three-electrode system (CE, SCE, and WE) was used to perform the electrochemical measurements. Glassy carbon electrode (GCE) was utilized as the working electrode. A GCE (diameter 3 mm) was sequentially polished using 1.0 and 0.3 μm alumina slurry, and then ultrasonically washed in double distilled and ethanol for one minute, respectively. The purified GCE was dried with nitrogen steam. The pSC_4-Au-NPs colloid was formed by different guest (ie, PQ-, dopamine, HMD-induced pSC_4-Au-NPs colloid, respectively). 100 μL of the prepared pSC_4-Au-NPs colloid was deposited on purified GCE, which was dried in an oven at about 50 °C for electrochemical experiments. The scanning potential range of CV was from 0.8 to –0.8 V at a scan rate of 50 mV/s in 0.1 M NaOH.

Apparatus and measurements

The UV–visible absorption spectra were recorded by a Shimadzu UV-2450 PC UV–visible spectrophotometer, with a path length of 10 mm and a volume of 50 μL quartz cuvette was implemented. The microstructures were observed using Nova NanoSEM 450 instrument. TEM was recorded on a JEM-2010F instrument with an operating accelerating voltage of 200 kV. The surface modification was coached by Fourier-transform infrared (FTIR) spectroscopy (JASCO, FTIR6300, Japan). The sample was centrifuged twice, drop-casted on a carbon coated copper grid, and dried under an infrared lamp. All electrochemical surveys were managed with an Autolab PGSTAT128N system (Eco Chemie B.V., the Netherlands). The modified GC electrode was used as the working electrode. Platinum foil and Ag/AgCl (1 M KCl) were introduced as the counter electrode and the reference electrode, respectively.

Results and Discussion

Characterization of the synthesized nanomaterials

The pSC_4-modified Au-network was directly synthesized by reduction of chloroauric acid with sodium borohydride in the presence of pSC_4 at room temperature. The produced pSC_4-Au-NPs were characterized with an average diameter of 5.0 ± 1.0 nm and the surface charge of −37.3 mV. Due to the anticipation of pSC_4, these NPs show good stability. It has been reported that diamine molecules can form a host-guest inclusion complex with pSC_4 in aqueous solution, and due to the strong affinity between the guest molecule and the Au core, it should also absorb and interact with the Au surface.[33] Therefore, some guest molecules can act as ligands to assemble pSC_4-Au-NPs into a network. The guest molecules were preferentially added and the pSC_4-Au-NPs solution of each sample was light red and stable for a minimum of three months. Gelation of the Au network is produced by introducing guest molecules into the solution. Addition of guest molecules to the pSC_4-Au-NPs solution initially resulted in prominent aggregation of pSC_4-Au-NPs, resulting in a change in colour from an initial light red to a purple or light gray. Our rendering method makes pSC_4-Au-NPs easy to gel by simply adding a sufficient amount of guest molecules.[34,35]

FTIR spectroscopy was used to monitor if Au-NPs were even capped by pSC_4. Fig. 1a shows the FTIR spectra of pSC_4 and Au-NPs modified with pSC_4. Collating the FTIR spectra of pSC_4 and pSC_4-AuNPs, valid features can be linked: the peaks for SO_3^- at 1049 cm^{-1} and 1187 cm^{-1}, as found in pSC_4, are shifted to 1035 cm^{-1} and1178 cm^{-1}, respectively, which advises that the SO_3^- groups concert with the Au atoms on the surface of the AuNPs.

In order to monitor the formation of the Au-network induced by the guest molecule, UV-visible spectroscopy was performed to measure the time-dependent growth (Fig. 1b and Supplementary Data, Fig. S1). After addition of PQ (0.5 mM), dopamine (0.6 mM) and HMD (0.7 mM), the surface plasmon resonance (SPR) peak of the pSC_4-AuNPs colloid decreases with a red shift from 513 to 524 nm. Suitable concentrations of different guest molecules have been studied by absorption spectroscopy (Figs 1c, 1d, 1e and Supplementary Data, Fig. S1). These usually indicate the formation of large-sized nanostructures compared to Au-NPs.[36] A gradual decrease in long wavelength SPR over time can be observed due to the stability of the large network structure. After overnight storing in room temperature, a stable Au-NPs network was synthesized at the bottom of the bottle.

After supercritical drying with CO_2, the three Au-network samples (formed by PQ, dopamine and HMD, respectively) proved almost identical to those

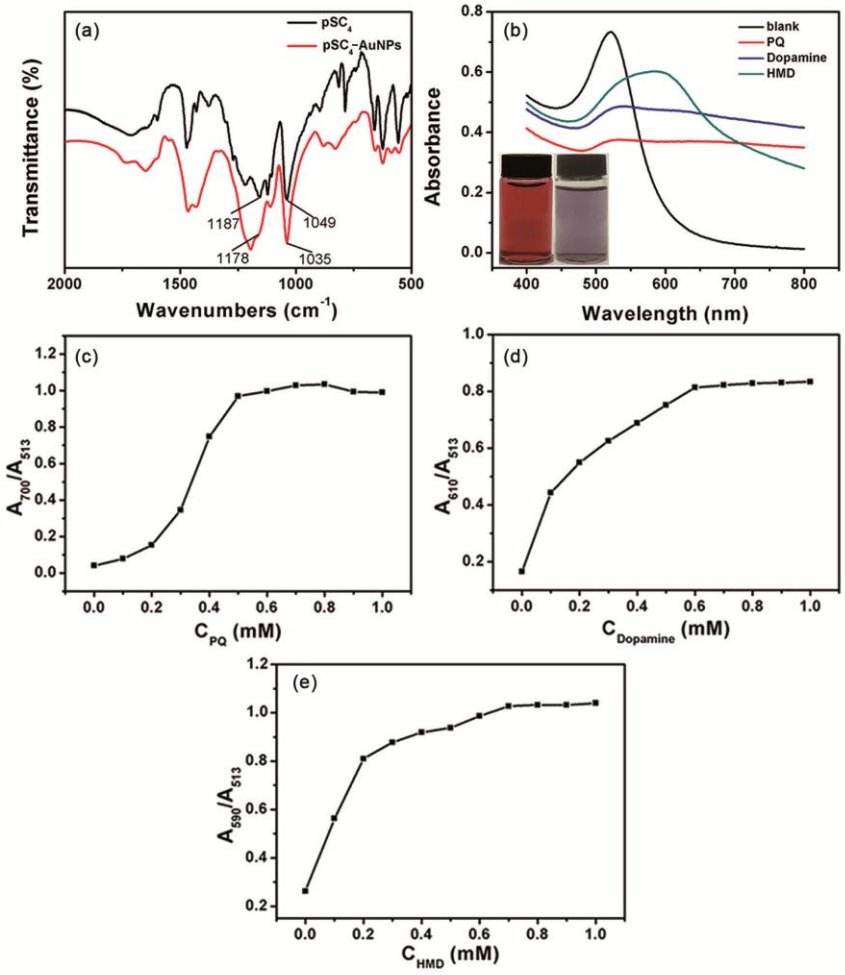

Fig. 1 — (a) FTIR spectra of the pSC_4-AuNPs, (b) UV−visible spectra for the pSC_4-AuNPs assembled by PQ (0.5 mM), dopamine (0.6 mM) and HMD (0.7 mM), Plots (c, d and e) for the pSC_4-Au-NPs assembled by PQ, dopamine and HMD (0−1 mM).

shown in scanning electron microscopy (SEM) and transmission electron microscopy (TEM) as shown in Fig. 2 and in Supplementary Data, Fig. S2. The expanding structure is highly porous and consists of an interconnected network of ultra-fine linear structures with many processes. They show a very pronounced pore size distribution with open macro and mesopores. The average diameter is similar to the size of the starting pSC_4-Au-NPs, so an immediate fusion of the original particles is proposed. The hierarchical porous structure of the Au-network having a large surface area can provide more reaction sites and enable rapid diffusion of the substrate in the catalyst.

We describe that the host-guest interaction between the guest molecule and pSC_4 may be one of the steering forces for the construction of the Au network by pSC_4-AuNPs. As shown in Fig. 2, three kinds of guest molecules of PQ, dopamine, and HMD, which were designated as PQ-pSC_4-Au-NPs, dopamine-pSC_4-Au-NPs, and HMD-pSC_4-Au-NPs, were introduced to the guest-induced assembly. PQ, dopamine and HMD are strongly bound to the surface of Au-NP and result Au-NPs networks. Representatively, PQ-pSC_4-Au-NPs and dopamine-pSC_4-Au-NPs result in uncontrolled aggregation.[33,37] In contrast, Au-NPs without guest remain unaltered initial size of AuNPs (6.0 ± 0.5 nm, Supplementary Data, Fig. S2). These results indicate that the guest-induced route achieves a simple, efficient way of 3D assembling Au-NPs. It not only provides a strategy for the production of high-quality Au networks, but also provides opportunities for further application in sensing, catalysis, surface-enhanced Raman spectroscopy, etc.

Electrochemical characterization of AuNPs networks

Due to the high selectivity and activity of the catalytic reaction, nanostructured Au materials have been utilized in sensing and catalysis.[2,30] On the other hand, nanostructured Au materials with multimodal porosity promote mass transfer and exhibit increased reaction sites and surface areas.[38-40] In this respect, the Au network with wide open porosity and high surface area prepared in this work was first tested as a preferred electrocatalyst for oxidizing glucose because it is of great importance for human health.[41,42]

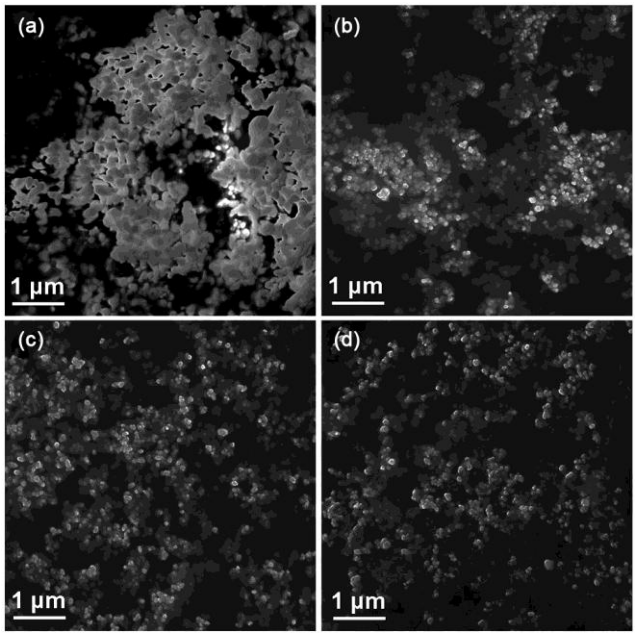

Fig. 2 — SEM images of (a) pSC_4-Au-NPs, and pSC_4-Au-NPs assembled by (b) PQ, (c) dopamine and (d) HMD.

As shown in Fig. 3a, all Au network modified GCEs (i.e., pSC_4-AuNPs/GCE, PQ-pSC_4-AuNPs/GCE, dopamine-pSC_4-AuNPs/GCE and HMD-pSC_4-AuNPs/GCE) depict electrochemical characteristics for Au in an alkaline solution, the anodization current starts around 0.20 V, which is due to the reduced structure of the Au oxide, as indicated by the reduction peak appearing in the negative potential scan. HMD-pSC_4-AuNPs/GCE showed the largest peak-to-peak potential separation, which means that the electrons transfer kinetics of the electrode surface is the fastest (Table 1). The larger electrochemically active surface area (ECSA) of the Au-network coupled to the HMD provides more active sites for further electrocatalytic reactions.

After adding different concentrations of glucose, in the positive potential scan with all Au-network modified GCEs, two anode peaks showed the oxidation of glucose. Further, an anode peak according to glucose oxidation is established in the

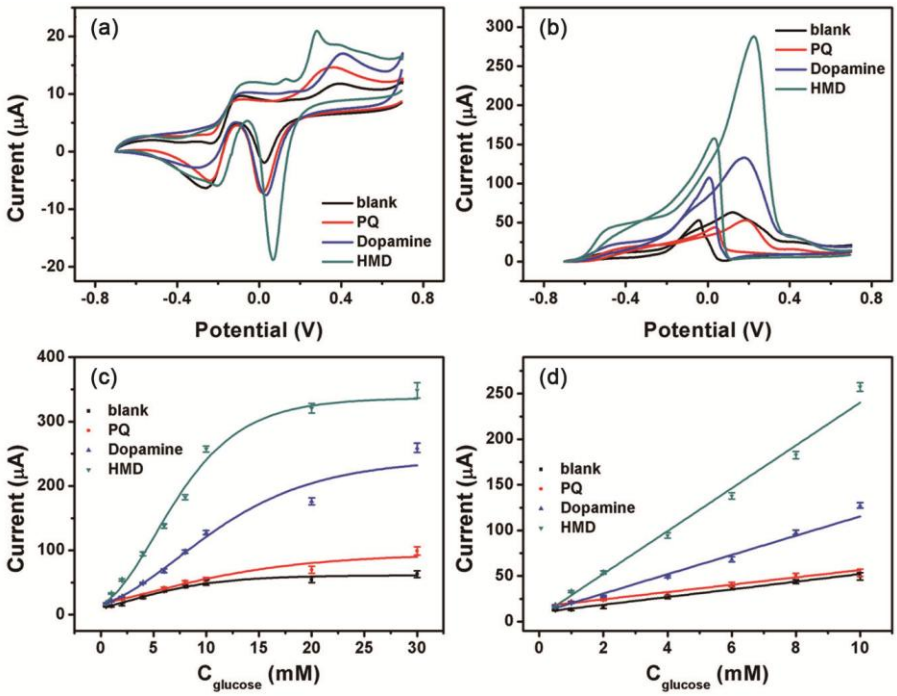

Fig. 3 — CVs of the pSC_4-Au-NPs, PQ-pSC_4-AuNPs, dopamine-pSC_4-Au-NPs and HMD-pSC_4-AuNPs modified electrodes (a) in the absence and (b) presence of 10 mM glucose in 0.1 M NaOH at a scan rate of 50 mV s^{-1}. Linear relationships of the electrocatalytic current of glucose *vs* concentration are shown in plot for (c) 0−30 mM and (d) 0−10 mM of the modified electrodes.

Table 1 — Electrochemical properties of the Au networks modified glassy carbon electrodes

Guest	ΔE_p (mV)	ΔI_p (μA)	ECSA ($m^2 g^{-1}$)	Slope	LOD (mM)
blank	0.37	13.7	10.7	4.20	0.220
PQ	0.35	21.8	12.2	4.01	0.374
Dopamine	0.37	24.6	13.8	10.58	0.142
HMD	0.21	39.8	17.1	23.48	0.076

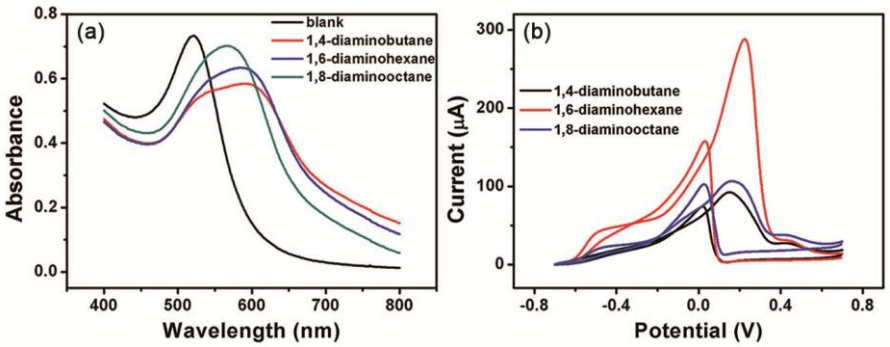

Fig. 4 — (a) UV−visible absorption spectra for the pSC_4-Au-NPs assembled by 1,4-diaminobutane, 1,6-diaminohexane and 1,8-diaminooctane. (b) CVs of the 1,4-diaminobutane-pSC_4-AuNPs (black line), 1,6-diaminohexane-pSC_4-Au-NPs (red line) (b) and 1,8-diaminooctane-pSC_4-Au-NPs (blue line) modified electrodes in the presence of 10 mM glucose in 0.1 M NaOH at a scan rate of 50 mV s^{-1}.

negative potential scan (Fig. 3b). The calibration curve according to the ampere response opposite to the glucose concentration is illustrated in Fig. 3c and 3d and in Supplementary Data, Fig. S3. HMD-pSC_4-Au-NPs/GCE showed very high activity in glucose oxidation with a sensitivity of 0.076 mM in the range of 0 to 10 mM, which is superior to those reported in the literature.[13,43-45] At the same time, control experiments show that all three Au-networks have much higher catalytic performance than the corresponding Au-NPs without nanostructure as an electrocatalyst (Fig. 3b). On the one hand, this is mainly because the Au-NPs network linked by the host and the guest increases the electrocatalytic conductance and electron transfer. On the other hand, the open porous structure of the Au-network not only provides the rapid transport of glucose through the electrolyte /electrode interface, but due to the high surface area, it also ensures contact with larger reaction surfaces.

ΔE_p is the difference of the anodic and cathodic peak potentials, ΔI_p is the current difference betweenthe oxidation peak and the reduction peak, and it is an important basis for judging whether the electrode reaction is a reversible system and shows the degree of reversibility of the electrochemical reaction. The ECSA values of GCE were calculated based on the following Randles–Sevcik equation.

$$i_p = 2.69 \times 10^5 n^{3/2} AD^{1/2} Cv^{1/2}$$

Where i_p = maximum current, n = number of electrons transferred in the redox event, A = electrode area in cm^2, D = diffusion coefficient in cm^2/s, C = concentration in mol/cm^3, v = scan rate in V/s. Its value indicates that it provides more active sites with higher catalytic performance. Slope refers to the ratio of current to different concentrations of glucose, the higher slope value showing higher reaction efficiency. LOD indicates that the HMD−pSC_4-AuNPs/GCE exhibits the highest activity and sensitivity upon glucose oxidation.

The size and distance between Au-NPs affect the electron transportatio efficiency through the electrolyte/ electrode interface. It is noted that the HMD mediated pSC_4-Au-NPs network shows the highest catalytic activities despite of the mass or specific current density. Consequently, diamine molecules of different chain lengths have been investigated in this system. As shown in Fig. 4a, the absorption spectra depict diamine molecules of different chain lengths mediated assembled pSC_4-Au-NPs networks. The suitable concentrations of different diamine molecules have been explored by UV-visible absorption spectra (Supplementary Data, Fig. S4). Three kinds of Au-network modified GCEs can result in electrocatalytic reaction but generated different peak currents. As shown in Fig. 4b, HMD-mediated assembled pSC_4-AuNPs networks modified GCEs still produce the greatest electrocatalytic effect. Own to the strong binding constant of HMD with

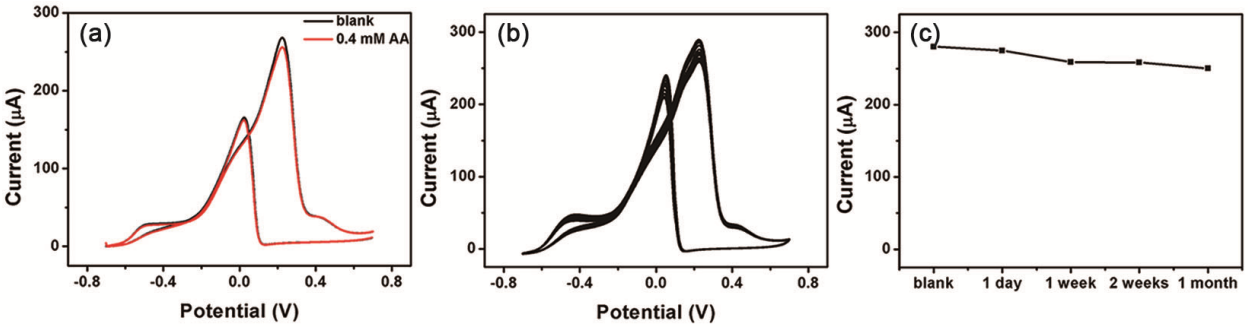

Fig. 5 — (a) CVs at the HMD-pSC_4-Au-NPs modified GCE in 10 mM glucose in 0.1 M NaOH solution before (black line) and after (red line) the addition of 0.4 mM ascorbic acid. The scan rate is 50 mV s^{-1}. (b) Corresponding curves of HMD-pSC_4-AuNPs modified electrodes response to different scan times in the presence of 10 mM glucose in 0.1 M NaOH at a scan rate of 50 mV s^{-1}. (c) Plots of the electrocatalytic current *vs* time of the modified electrodes.

pSC_4 and the relative molecular flexibility comparing with that of PQ, DA and other two diamine molecules (n=4, 8), HMD mediated the aggregation of pSC_4-Au-NPs has the biggest effective surface area and fast electron transformation. Thus, HMD-pSC_4-Au-NPs modified electrode shows the best enzymatic activity.

Sensitivity, reproducibility and stability of the proposed sensor

To assess sensor selectivity, ascorbic acid is often selected as an interfering molecule for glucose sensing because of their similar chemical properties. However, the pSC_4-Au-NPs network modified electrode showed a slight electrochemical response to 0.4 mM ascorbic acid (Fig. 5a). In order to measure the reproducibility and stability of the sensor, after 15 consecutive scans, the Au network modified electrode showed an initial catalytic current of more than 93.6%, and almost no change after storage for one month at room temperature until glucose oxidation (Fig. 5b and 5c). Although pSC_4-AuNPscan only catalyze glucose in an alkaline environment, which may limit the practical application of this method, these results indicate that the Au network has high sensitivity, wide linear range and good stability, demonstrating the prospect of HMD-pSC_4-Au-NPs/GCE as a non-enzymatic sensitive electrode for analytical applications.

Conclusions

In short, we successfully built a new, convenient Au-network component through a guest-guided route. Interestingly, different guest molecules induce different Au-NPs network structures, resulting in their different oxidative abilities to glucose. The HMD-pSC_4-Au-NPs network modification electrode is implemented in electrocatalysis, providing high activity for non-enzymatic oxidation of glucose, which provides a high-performance glucose sensor. The synthesis procedure is characterized by a simple, fast and versatile polymerization of NPs. Due to the high surface area and increased conductance and electron transfer, this approach provides a platform for the development of more stable and efficient glucose sensors based on supramolecular mediated Au-NPs networks.

Supplementary Data

Supplementary Data associated with this article are available in the electronic form http://nopr.niscair.res.in/jinfo/ijca/IJCA_59A(10)1434-1441_SupplData.pdf.

Acknowledgement

This work was supported by the National Natural Science Foundation of China (No. 61275085) and the Open Project Program of State Key Laboratory of Dairy Biotechnology (No. SKLDB2016-001).

References

1 Boal A K, Ilhan F, DeRouchey J E, Thurn-Albrecht T, Russell T P & Rotello V M, *Nature*, 404 (2000) 746.
2 Wang F A, Liu X Q & Lu C H, *ACS Nano*, 7 (2013) 7278.
3 Nie Z H, Petukhova A & Kumacheva E, *Nat Nanotechnol*, 5 (2010) 15.
4 Yue M L, Li Y C, Hou Y, Cao W X, Zhu J Q, Han J C, Lu Z Y & Yang M, *ACS Nano*, 9 (2015) 5807.
5 Stevens M J, *Science*, 343 (2014) 981.
6 Tan L H, Xing H & Lu Y, *Acc Chem Res*, 47 (2014) 1881.
7 Ma G X, Zhou Y L, Li X Y, Sun K, Liu S Q, Hu J Q & Kotov N A, *ACS Nano*, 7 (2013) 9010.
8 Gao M R, Zhang S R, Xu Y F, Zheng Y R, Jiang J & Yu S H, *Adv Funct Mater*, 24 (2014) 916.
9 Mohanan J L, Arachchige I U & Brock S L, *Science*, 307 (2005) 397.
10 Gaponik N, Herrmann A K & Eychmüller A , *J Phys Chem Lett*, 3 (2012) 8.

11 Olsson R T, Azizi Samir M A S, Salazar-Alvarez G, Belova L, Ström V, Berglund L A, Ikkala O, Nogués J & Gedde U W, *Nat Nanotechnol*, 5 (2010) 584.
12 Okesola B O, Suravaram S K, Parkin A & Smith D K, *Angew Chem*, 128 (2016) 191.
13 Wen D, Liu W, Haubold D, Zhu C Z, Oschatz M, Holzschuh M, Wolf A, Simon F, Kaskel S & Eychmüller A, *ACS Nano*, 10 (2016) 2559.
14 Oezaslan M, HaschéF & Strasser P, *J Phys Chem Lett*, 4 (2013) 3273.
15 Willner I & Willner B, *Nano Lett*, 10 (2010) 3805.
16 Yu A, Liang Z, Cho J & Caruso F, *Nano Lett*, 3 (2003) 1203.
17 Tsukamoto D, Shiraishi Y, Sugano Y, Ichikawa S, Tanaka S & Hirai T, *J Am Chem Soc*, 134 (2012) 6309.
18 Tang Y & Cheng W, *Langmuir*, 29 (2013) 3125.
19 Wei T X, Dong T T, Wang Z Y, Bao J C, Tu W W & Dai Z H, *J Am Chem Soc*, 137 (2015) 8880.
20 Young S L, Kellon J E & Hutchison J E, *J Am Chem Soc*, 138 (2016) 13975.
21 Li H, Chen D X, Sun Y L, Zheng Y B, Tan L L, Weiss P S & Yang Y W, *J Am Chem Soc*, 135 (2013) 1570.
22 Liu W, Herrmann A K, Bigall N C & Rodriguez P, *Acc Chem Res*, 48 (2015) 154.
23 Gao X N, Esteves R J, Luong T T H, Jaini R & Arachchige I U, *J Am Chem Soc*, 136 (2014) 7993.
24 Alkilany A M, Lohse S E &Murphy C J, *Acc Chem Res*, 46 (2013) 650.
25 Howes P D, Chandrawati R & Stevens M M, *Science*, 346 (2014) 1247390.
26 Zhang Y, Cui X J, Shi F & Deng Y Q, *Chem Rev*, 112 (2012) 2467.
27 Bigall N C, Herrmann A K, Vogel M, Rose M, Simon P, Carrillo-Cabrera W, Dorfs D, Kaskel S, Gaponik N & Eychmüller A, *Angew Chem Int Ed*, 48 (2009) 9731.
28 Liu W, Herrmann A K, Geiger D, Borchardt L, Simon F, Kaskel S, Gaponik N & Eychmüller A, *Angew Chem Int Ed*, 51 (2012) 5743.
29 Lin Y H, Ren J S & Qu X G, *Adv Mater*, 26 (2014) 4200.
30 Tang M Y, Chen S H, Yuan R, Chai Y Q, Gao F X & Xie Y, *Anal Sci*, 24 (2008) 487.
31 Dhara K & Mahapatra D R, *Microchimi Acta*, 185 (2018) 49.
32 Masitas R A, Allen S L & Zamborini F P, *J Am Chem Soc*, 138 (2016) 15295.
33 Park J W & Shumaker-parry J S, *J Am Chem Soc*, 136 (2014) 1907.
34 Wang X, Koh K & Chen H, *Sens Actuators B*, 251 (2017) 869.
35 Wang X, Du D, Dong H, Song S, Koh K & Chen H, *Biosens Bioelectron*, 99 (2018) 375.
36 El-Sayed M A, *Acc Chem Res*, 34 (2001) 257.
37 Kisner A , Heggen M , Fernández E , Lenk S, Mayer D, Simon U , Offenhäusser A & Mourzina Y, *Chem Eur J*, 17 (2011) 9503.
38 He W H, Jiang C H, Wang J B & Lu L H, *Angew Chem Int Ed*, 53 (2014) 9503.
39 Kajdos A, Kvit A, Jones F, Jagiello J & Yushin G, *J Am Chem Soc*, 132 (2010) 3252.
40 Xia W, Zou R Q, An L, Xia D G & Guo S J, *Energy Environ Sci*, 8 (2015) 568.
41 Zhu C Z, Guo S J & Dong S J, *Adv Mater*, 24 (2012) 2326.
42 Kwon K H, Lee S H, Choi Y B, Lee J A, Kim S H, Kim H H, Spinks G M, Wallace G G, Lima M D, Kozlov M E, Baughman R H & Kim S J, *Nat Commun*, 5 (2014) 3928.
43 Jena B K & Raj C R, *Chem Eur J*, 12 (2006) 2702.
44 Liu A P, Ren Q H, Xu T, Yuan M & Tang W H, *Sens Actuators B*, 162 (2012) 135.
45 Plowman B J, O'Mullane A P, Selvakannana P R & Bhargava S K, *Chem Commun*, 46 (2010) 9182.